IEEE Photonics Journal
An IEEE Photonics Society Publication

Open Access

Performance of Injection-Locked Quantum-Dash MMW Source Under Clear and Dusty Weather Conditions

Volume 13, Number 3, June 2021

Qazi Tareq
Amr Mohamed Ragheb
Maged Abdullah Esmail
Saleh Abdullah Alshebeili
Mohammed Zahed Mustafa Khan

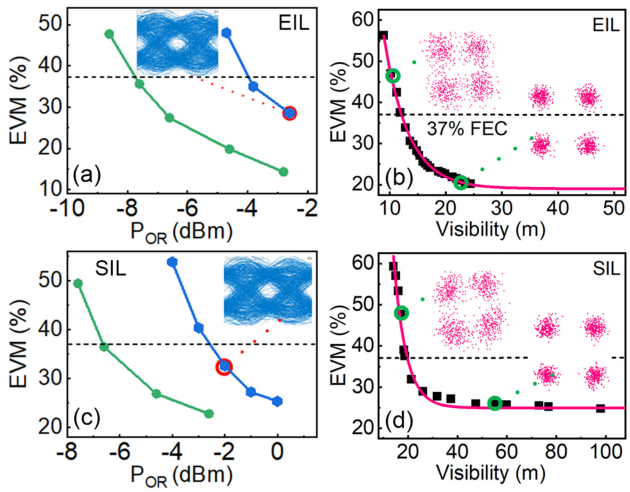

DOI: 10.1109/JPHOT.2021.3074425

Performance of Injection-Locked Quantum-Dash MMW Source Under Clear and Dusty Weather Conditions

Qazi Tareq,[1] Amr Mohamed Ragheb,[2,4] Maged Abdullah Esmail,[3] Saleh Abdullah Alshebeili,[4] and Mohammed Zahed Mustafa Khan[1]

[1]Optoelectronics Research Laboratory, Electrical Engineering Department, King Fahd University of Petroleum and Minerals (KFUPM), Dhahran 31261, Saudi Arabia
[2]KACST-TIC in Radio Frequency and Photonics for the e-Society (RFTONICS), King Saud University (KSU), Riyadh 11421, Saudi Arabia
[3]Communications and Networks Engineering Department and Smart Systems Engineering Laboratory, Prince Sultan University, Riyadh 11586, Saudi Arabia
[4]Electrical Engineering Department, King Saud University (KSU), Riyadh 11421, Saudi Arabia

DOI:10.1109/JPHOT.2021.3074425

Manuscript received April 15, 2021; accepted April 16, 2021. Date of publication April 21, 2021; date of current version May 3, 2021. The work of Qazi Tareq and Mohammed Zahed Mustafa Khan was supported by Deanship of Research at King Fahd University of Petroleum and Minerals (KFUPM) under Grant SB181003. The work of Amr Mohamed Ragheb and Saleh Abdullah Alshebeili was supported by the National Plan for Science, Technology, and Innovation (MAARIFAH), King Abdulaziz City for Science and Technology, Kingdom of Saudi Arabia, under Award 2-17-02-001-0009. The work of Maged Abdullah Esmail was supported by Prince Sultan University. Corresponding author: Mohammed Zahed Mustafa Khan (e-mail: zahedmk@kfupm.edu.sa).

Abstract: We report on the generation and transmission of 30 GHz millimeter-wave (MMW) beat-tone signals employing external- (EIL) and self-injection-locked (SIL) InAs/InP quantum-dash based dual-wavelength laser (QD-DWL) sources emitting in mid L-band. Later, successful transmission of 2 Gbps quadrature phase-shift-keying (QPSK) signal over clear weather conditions on 2 m wireless (WL), and hybrid channels consisting of 20 km single-mode fiber (SMF) and 2 m WL, and 20 km single-mode fiber (SMF), 5 m free-space-optics (FSO) and 2 m WL, are demonstrated employing both MMW sources, with a slight $\sim$1.4 dBm extra received optical power requirement from SIL QD-DWL. Lastly, examining the effect of dusty weather conditions on the MMW transmission over 20 km SMF, 0.9 m FSO and 1 m WL hybrid channel, considering both EIL and SIL sources, showed maximum visibility range (V) of 12 $\pm$ 2 m and 16 $\pm$ 2 m for successful transmission, respectively. These investigations reinforce the simple, cost-effective, and energy-efficient SIL QD-DWL as a candidate L-band millimeter-wave (MMW) source compared to the EIL counterpart in 5G and next-generation radio-over-fiber wavelength-division multiplexing networks.

Index Terms: Quantum-dash laser, injection locking, millimeter waves, radio-over-fiber, optical communications, dusty weather.

1. Introduction

Fifth-generation (5G) wireless communication networks have already been deployed in several countries across the globe to satiate exponential growth of mobile traffic data (77 Exabytes/ month by 2022) [1]. Nevertheless, to provide ubiquitous connectivity, 5G is facing major challenges to ascertain 10 Gbps maximal throughput and ultrafast transfer while assuring ultra-low 1 ms latency

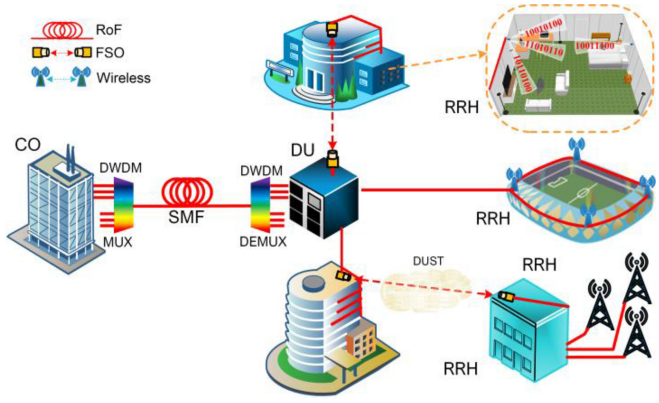

Fig. 1. Concept analog optical fronthaul architecture for 5G applications. DU: distributed unit, CO: central office, DWDM: dense wavelength-division multiplexing, RRH: remote radio head, RoF: radio-over- fiber, FSO: free-space-optics, SMF: single-mode fiber.

[2]. To expedite these tasks, the millimeter-wave (MMW) transmission window (24.25–52.6 GHz) has been proposed for emerging 5G architecture. However, owing to the atmospheric attenuation that limits MMW wireless (WL) propagation for longer distances, pico-cells with 40-50 base stations/km^2 [3] have been proposed, and typically getting integrated with the existing fiber network infrastructure, commonly referred to as radio-over-fiber (RoF). This hybrid MMW architecture is garnering recent attention and perceived as a potential network to deliver broadband services at 28–39 GHz, and even incorporating free-space-optics (FSO) with reduced atmospheric attenuation [4]. For illustration purpose, a conceptual optical fronthaul architecture has been shown in Fig. 1, where MMW carrier signals are generated and multiplexed in the central office (CO) to be transmitted over single-mode fiber (SMF) to a distribution unit (DU). After demultiplexing various received MMW carriers, the DU routes each signal directly to the designated remote radio head (RRH). The architecture also reveals potential hybrid channels, such as RoF-WL and RoF-FSO-WL, promising for the next-generation optical networks. In particular, areas where fiber installation is non-trivial, FSO could be used as a potential solution [5], offering fundamental advantages such as license-free bandwidth and seamless integration with existing fiber infrastructure. However, FSO channels are prone to weather conditions (*i.e.,* signal attenuation and distortion due to humidity, fog, snow, dust, etc.) as illustrated in Fig. 1, which could severely degrade the system performance, and its effect in hybrid RoF-FSO-WL networks is of paramount importance to ascertain their practical deployability.

In literature, most RoF-FSO investigations are focused on fog, air-turbulence, humidity, etc. [1], [2]. For instance, in [6], a comparison of tera-hertz with near-infrared 1550 nm intensity modulated (IM) signals over dusty FSO link showed the latter source suffering two orders of magnitude higher attenuation than the former one. On the other hand, reference [7] demonstrated that 830 nm light source showed superior performance than 760 nm when analyzed under combined effects of dust and turbulence. In [8], an empirical signal attenuation model for 1550 nm source from dusty weather FSO link experiments under a controlled dust chamber is reported. Subsequently, the authors analyzed 28 GHz 1550 nm RoF-FSO link carrying 4 Gbps 16-quadrature amplitude modulation (16-QAM) 5G signal and found 50 m as the visibility range (V) threshold to maintain forward-error-correction (FEC) limit under dense dust storm conditions [5]. However, a rigorous analysis of such hybrid network infrastructure under dusty conditions and employing MMW carriers generated by mid and far L-band wavelength optical sources is not reported yet, to the authors' knowledge, which is an essential step since next generation optical networks are considering wavelength operation beyond C-band region.

Besides channel characteristics, another crucial aspect for coherent WL, RoF-WL, or RoF-FSO communication is the photonics generation of MMW signal with low phase noise and narrow

linewidth to ascertain low-latency transmission [9]. In this regard, quantum confined nanostructure-based semiconductor lasers, in particular, InAs/InP quantum-dash (QD) laser diode (QD-LD), is garnering great interest as promising MMW sources, thanks to their high-performance characteristics compared to other active region counterparts [10], [11]. For instance, a 3-20 GHz microwave/MMW signal was initially demonstrated utilizing a 1550 nm QD distributive feedback (DFB) dual-wavelength laser (DWL) [12]. Later, in references [13] and [14], generation of 46 and 48 GHz MMW from this QD DWL and subsequent transmission of 2 Gbps 4-level pulse amplitude modulation (PAM) is reported. Moreover, passively mode-locked QD-LD at 1550 nm [15] has also been exploited for 60 GHz MMW generation and transmission, thanks to the high coherency between the optical tones that enable 1.58 Gbps quadrature phase-shift-keying (QPSK) transmission over 3m WL channel. Besides, a 25 Gb/s 16-QAM orthogonal frequency division multiplexing (OFDM) signal over 60 GHz MMW carrier is also demonstrated on a 50 km RoF channel employing gain-switched DFB laser-based optical frequency comb [16]. However, all QD-LD demonstrations are in the classical C-band wavelength. Hence, very recently, exploiting the dash emission tunability during the growth process, we recently demonstrated the possibility of generation and unmodulated transmission of 28, 38, and 60 GHz, MMW carrier over WL channel, employing $\sim$1610 nm QD-LD in the challenging mid L-band window [11]. These preliminary results, exploiting niche dash wavelength tunability feature, make L-band QD-LD a promising MMW source for next-generation L-bands networks, integrating hybrid RoF-FSO-WL technologies, and preserving colorless operation via potential injection locking technique in RoF wavelength division multiplexed (WDM) networks.

In this work, we aim to substantiate further the outlook of QD-LD as a potential MMW source by (i) investigating the transmission performance of 2 Gbps QPSK modulated 30 GHz MMW beat-tone carrier generated by $\sim$1610 nm QD dual-wavelength laser (QD-DWL) under clear (C, indoor laboratory environment) weather conditions and (ii) dusty (D, laboratory chamber with controlled dust environment) weather conditions, which to the authors' knowledge, has not been reported yet in the L-band region; and (iii) comparing the MMW transmission performance of external- (EIL) and self-injection-locked (SIL) based QD-DWL under both weather conditions. In general, EIL QD-DWL showed slightly better performance ($\sim$1.4 dBm better optical receiver sensitivity) compared to SIL case under various WL and hybrid RoF-WL and RoF-FSO-WL channels under clear weather conditions. Moreover, under a dusty weather environment with a 20 km SMF - 0.9 m FSO - 1 m WL hybrid channel, a receiver forward error correction (FEC) limit is noted at $V = 12 \pm 2$ m and 16 ± 2 m from EIL and SIL based QD-DWL, respectively, again demonstrating similar performance. This is the first report of modulated MMW transmission performance comparing injection-locked QD-LD in the mid L-band region to the authors' knowledge.

2. Experimental Setup

The experimental setup is depicted in Fig. 2(a). An in-house fabricated and cleaved QD-LD based DWL (QD-DWL) source, reliant upon optical injection, is employed, exhibiting 35 GHz free-spectral range or mode spacing. These modes are then injected into a single drive Mach-Zehnder modulator (MZM) and externally modulated with a 2 Gbps QPSK signal at an intermediate carrier frequency (IF) of 5 GHz. The modulated 30 GHz MMW photonic signal beat-tone at the output of MZM is then amplified (OA1, AEDFA-L-EX2-B-FA) to compensate for the modulator insertion loss before passing through a 20 km SMF and then either to a dusty FSO (FSOD, 0.9 m chamber) or clear FSO (FSOC, 5 m indoor) link and received via a 70-GHz photodetector (PD, Finisar XPDV3120) after passing through a variable optical attenuator (VOA). The PD generates all possible MMW signals due to beating between two optical carriers, optical carrier and sideband, and two sidebands (10, 30, 35, 40, 45 GHz) due to double sideband modulation. However, all frequencies except 30 GHz (modulated) and 35 GHz (unmodulated) carrier signal are automatically eliminated after passing through a low noise amplifier (LNA, Quinstar QLW-24403336 bandwidth 24-40 GHz), owing to its limited bandwidth operation. Next, these MMW signals are transmitted and received via two identical 25 dBi gain horn antennas before being down-converted by a mixer with a 30.5 GHz local

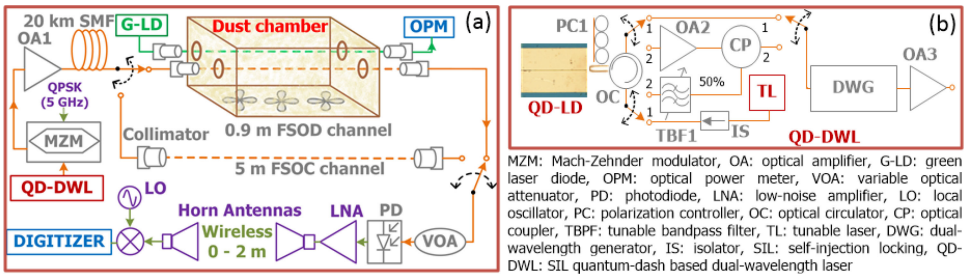

Fig. 2. Experimental setup for (a) MMW transmission over 20 km SMF, FSO and 0-2 m WL hybrid channel. For clear and dusty weather conditions, the FSO channel length is 5 m and 0.9 m, respectively. (b) QD-DWL source where terminals 1 and 2 correspond to single mode generation of QD-LD emitting at ∼1610 nm, using EIL and SIL schemes, respectively.

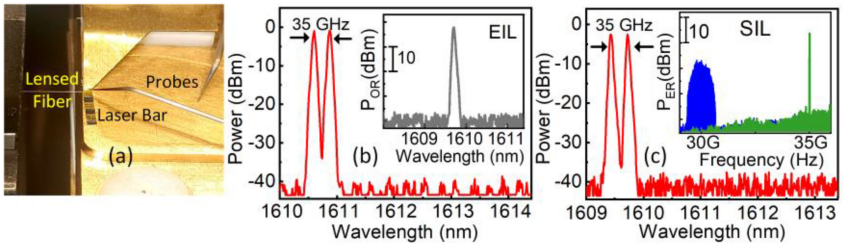

Fig. 3. (a) Zoomed photograph of the bare QD- LD whose single-facet power is coupled to a lensed SMF. Dual wavelength modes of QD-DWL, with 35 GHz free-spectral range, employing (b) EIL and (c) SIL techniques, and exhibiting 2% of actual power, obtained using optical spectrum analyzer with 60 pm resolution bandwidth. The inset of (b) shows single EIL mode at ∼1610 nm with 35 dB SMSR and (c) shows heterodyned 35 and 30 GHz MMW electrical beat-tones from the SIL QD-DWL. The insets have arbitrary units.

oscillator (LO) to retrieve the original signal, which is then analyzed on a digitizer (12-bit Keysight M9730B).

The FSOC and FSOD links, depicted in Fig. 2(a), are laboratory built whose details could be found elsewhere [5], [8]. In brief, the FSOC channel consists of two fiber collimators in tandem, separated by 5 m. On the other hand, the FSOD channel comprises a 90 $\times$ 40 $\times$ 40 cm^3 chamber with uncoated transparent windows for the optical signal to travel through. The chamber allows creating a controlled dust environment, emulating outdoor dust storms. The dust particles used are distributed homogenously by blowing arrays of fans installed at the bottom. These dust particles were collected from natural dust storms exhibiting an average size of 17.3 μm [5]. Since the performance communication system under dusty weather condition is evaluated in term of *V*, hence, to calculate *V*, another FSO link parallel to the first link (*i.e.,* for QD-DWL signal), as shown in Fig. 2(a), was constructed with a 550 nm green laser source (G-LD, Thorlabs S3FC520) and collimators. The received green signal is connected to an optical power meter (OPM) which measures the received optical power.

Lastly, the details of the QD-DWL source are illustrated in Fig. 2(b). The bare 4$\times$800 μm^2 InAs/InP QD-LD is a four stack chirped barrier thickness InAs dash in InGaAlAs well structure. The as-cleaved device is operated under a fixed continuous-wave current of 170 mA (1.78I_{th}) and a temperature-controlled environment, whose one-facet output power is butt-coupled into an in-house made lensed SMF with ∼0.5 mW fiber-coupled power as shown in Fig. 3(a). When the output of QD-LD is connected to terminal 1, EIL is realized (*i.e.,* via tunable laser, TL, isolator, IS, and optical coupler, OC), whereas switching to terminal 2 results in SIL (achieved via OC, optical amplifier OA2, -3 dB coupler, CP2, and TBF1). More details of the injection locking setup could

TABLE 1
Optical Received Power Level Measured at FEC for Error Free Transmission on Various Channels

	Receiver Sensitivity (dBm)					
	Wireless		Hybrid-WL		Hybrid –FSO	
	0m	2m	0m	2m	0m	2m
EIL	-9.0	-4.4	-8.5	-4.0	-7.7	-4.0
SIL	-7.0	-3.4	-6.6	-3.0	-6.6	-2.6

±0.25 dBm error margin.

be found elsewhere [10]. Utilizing either of these techniques, a single Fabry-Perot (FP) mode at ∼1610 nm is locked as shown in the inset of Fig. 3(b) to improve the coherency of the mode. Next, a dual-wavelength lasing emission is obtained by passing through a dual-wavelength generator (DWG) composed of a polarization controller, phase modulator driven by 35 GHz electrical signal and tunable bandpass filter, and later amplified by an optical amplifier (OA3) to compensate for various insertion losses. The dual-mode lasing of the EIL and SIL QD-DWL with >35 dB optical signal to noise ratio is depicted in Fig. 3(b) and (c), respectively. It is to be noted here that Fig. 2(b) could essentially be replaced by a single-section passively mode-locked QD-LD device should mode-locking be witnessed in mid L-band, which, unfortunately, has not been observed yet. This would potentially open a new paradigm of exploiting multiwavelength ∼1610 nm lasing emission of the mode-locked QD-LD to supply several dual modes MMW sub-carriers in RoF, RoF-WL, and RoF-FSO-WL based future WDM networks.

3. Results and Discussion

First, the dual optical carriers, depicted in Fig. 3(b) and (c), which are externally DSB modulated, are beaten at the PD to generate both 35 GHz unmodulated, and 30 GHz modulated MMW carriers, as shown in the inset of Fig. 3(c), employing both EIL and SIL QD-DWL. Next, the corresponding modulated MMW beat-tones, which exhibited low phase noise and narrow linewidths, are engaged to assess and compare the transmission performance under clear and dusty weather conditions using various practical channel combinations. As mentioned earlier, three different channel links; L_1: WL (0-2 m), L_2: HY (20 km SMF and 0-2 m WL), and L_3: HY-FSO (20 km SMF, 5 m FSOC, and 0-2 m WL), have been set up under laboratory environment to emulate and evaluate clear weather conditions. On the other hand, the performance on the dusty weather condition has been conducted on channel link L_4 (20 km SMF, 0.9 m FSOD and 1 m WL) that includes utilizing the chamber, as shown in Fig. 2. Furthermore, while conducting transmission experiments, identical optical power is maintained from both sources before transmitting through L_1, L_2, and L_3 channels for clear weather conditions. On the other front, for dusty weather conditions, 0 dBm optical power is assured at the dust chamber's input by adjusting the optical power before the SMF transmission accordingly. In all cases, error vector magnitude (EVM) at the receiver is measured by varying the optical received power (P_{OR}) using VOA along with parameters such as constellation, eye diagram, electrical received power, and SNR. A successful performance measure for coherent reception is determined at an average EVM of 37% for QPSK, translating to FEC bit error rate (BER) of 3.8×10^{-3}. This has been employed as a Fig. of merit for QPSK transmission system assessment [17], [18]. Furthermore, the BER is calculated from the EVM following reference [19].

3.1 Transmission Under Clear Weather Conditions

The results of transmission quality for the 2 Gbps QPSK modulated 30 GHz MMW carrier over L_1, L_2, and L_3 channels under clear weather conditions are plotted in Figs. 4 (a)–(c) and Figs. 4 (d)–(f), for EIL and SIL QD-DWL, respectively, whereas the corresponding measured receiver sensitivity (P_{OR} at 37% EVM for QPSK) are summarized in Table 1. Under the influence of L_1, P_{OR} required for

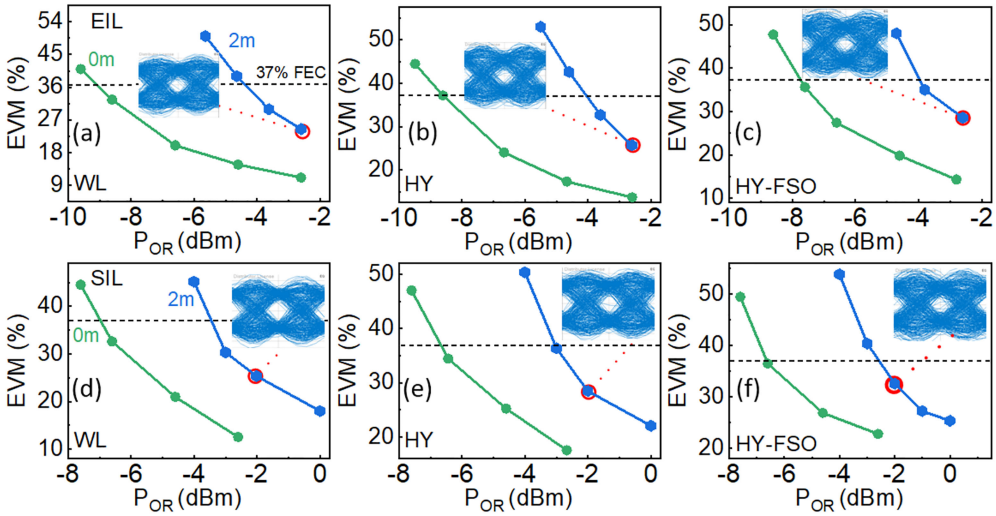

Fig. 4. Transmission performance of (a)–(c) EIL and (d)-(f) SIL QD-DWL under clear weather condition. EVM versus P_{OR} for 2Gbps QPSK modulated 30 GHz MMW carrier over channel links (i) L_1: WL (0–2 m), (ii) L_2: HY (20 km SMF and 0-2 m WL), and (iii) L_3: HY-FSO (20 km SMF, 5 m FSOC and 0-2 m WL). The respective insets show the eye diagram at the corresponding P_{OR}.

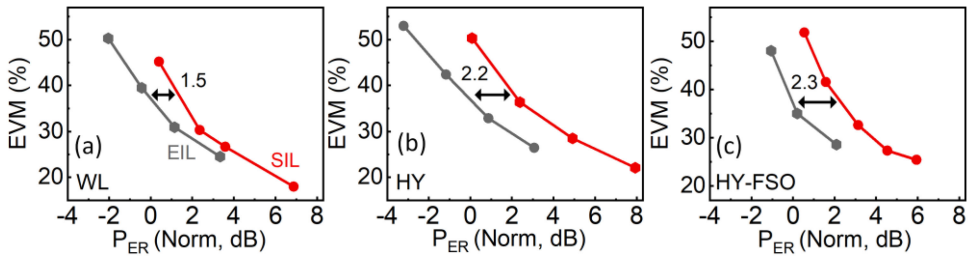

Fig. 5. EVM versus P_{ER} for the EIL and SIL QD-DWL at the same received P_{ER}, and normalized (Norm)to the FEC P_{ER} of the EIL-QD-DWL, over various channels (a) L_1: WL (2 m), (b) L_2: HY (20 km SMF and 2 m WL), and (c) L_3: HY-FSO (20 km SMF, 5 m FSOC and 2 m WL). The numbers in (a)–(c) shows the P_{ER} difference between EILand SIL QD-DWL in dB and at FEC EVM of 37%.

error-free transmission at 0 m WL distance for SIL QD-DWL is slightly larger by 2.0 dBm compared to EIL counterpart. In fact, a similar trend is also observed from these sources across L_2 and L_3 links, exhibiting an FEC POR difference of $\sim$1.9 and $\sim$1.1 dBm, respectively, and for the 2m WL distance ($\sim$1.0-1.4 dBm disparity). This constitutes an average $\sim$1.4 dBm extra power requirement by SIL QD-DWL to reach FEC compared to EIL. To ascertain this finding, Fig. 5(a)–(c) depicts the EVM as a function of the same received electrical power (P_{ER}) by both the sources but normalized to the FEC value of EIL QD-DWL for L_1, L_2, and L_3 at 2m WL distance. As expected, PER difference of $\sim$1.5-2.3 dBm, corresponding to a mean value of $\sim$2.0 dBm, is noted between the performance of SIL and EIL QD-DWL sources, or in other words, SIL based source again displayed a minor difference of PER compared to EIL counterpart, and consistent with the P_{OR} observation. This suggests a slightly lower quality 30 GHz MMW beat signal of SIL QD-DWL and attributed to the source's relative-intensity noise (RIN). As it has been shown in the literature that RIN plays a role in increasing the noise level of the generated MMW beat-tone [15], the RIN of EIL QD-DWL follows that of the high-quality tunable laser (Keysight 81600B) source that exhibited ~ -145 dB/Hz, and SIL-DWL should follow this value as the device structure design is unoptimized. Nevertheless, the advantages of a cost-effective and simple solution for next-generation optical networks offered

TABLE 2
Performance of QD-DWL MMW Sources Under Dusty Weather Conditions

	Dense (<0.2 km)		Moderate (0.2-1 km)		Clear (Before Start)	
	EIL	SIL	EIL	SIL	EIL	SIL
V (m)	12±2	16±2	-	-	-	-
P_{ER} (dBm)	-49 [a]	-50 [a]	-43 [a]	-45 [a]	-41 [a]	-42 [a]
EVM (%)	37	37	19	23	17.5	18.6
-log(BER)	2.42	2.42	7.8	4.4	7.8	6.0

[a] ±1 dBm error margin

by SIL QD-DWL (i.e., eliminating tunable laser, OA2 by efficient QD-LD fiber power coupling, and TPF1 by tunable fiber-Bragg-Gratings) outweigh this slight decrease in performance. It is also worth mentioning here that the QD-LD are un-optimized specimens, and hence an optimized design may help decrease the RIN further. Next, comparing receiver sensitivity of L_1 with L_2, and L_2 with L_3, at 0 m WL length, summarized in Table 1, for both EIL and SIL QD-DWL sources, a difference of ∼0.4 dBm average value is observed. Moreover, this value is consistent even at 2 m WL length and suggests a small contribution of 20 km SMF and 5 m FSO channels on the transmission performance. This minor difference is ascribed to the chromatic dispersion induced slight decorrelation of the two optical tones for L_2 [16] and possible measurement variation owing to FSO fiber collimators alignment for L_3. Nevertheless, an error-free transmission is achieved across all channels that could also be affirmed with open eye diagrams in Fig. 4. It is to be noted that the WL and FSO channel distances are limited by the constraints of the indoor laboratory space and not because of the QD-DWL sources.

3.2 Transmission Under Dusty Weather Condition

Next, the SIL and EIL QD-DWL based MMW source performance under dusty weather conditions is investigated by measuring the transmission characteristics over the L_4 channel link, firstly, with the clear chamber (before start). The results are tabulated in Table 2. Next, fans are turned on for a while to ensure homogenous distribution of dust across the chamber. Then, the data at the receiver was collected for 40 min with 30-sec interval. In this analysis, *V* is considered as a measure of severity of the dust storm where lower visibility range indicates high dust particle concentration in the atmosphere. Based on the range of *V*, two dust event categories are selected for performance comparison and are presented in Table 2. The range of *V* can be calculated as *V* (km) = -0.07/[10 log *T*], where *T* is the transmittance, which is the difference between experimentally received 550 nm green-LD power under dusty weather condition and the clear case (*i.e.,* before start), at any time interval [5]. Hence, the green-LD, whose input power was fixed at 4 dBm (measured at the input of the chamber), is also simultaneously turned on along with the QD-DWL MMW source and ran till 40 min, while the received power at the output of the chamber was noted via OPM [5]. The experiment is repeated by deploying the EIL QD-DWL source first and then SIL QD-DWL. The results are plotted in Fig. 6(a)–(c) for the EIL QD-DWL 2 Gbps QPSK modulated 30 GHz MMW source, whereas Fig. 6(d)–(f) depicts the performance of the SIL counterpart over the L_4 link. In particular, the performance is evaluated in terms of EVM, BER, and P_{ER}, as a function of *V*, as shown in Fig. 6. Under dense dust conditions, the EIL QD-DWL source based transmission system achieved an EVM limit of 37% for the successful transmission of 2 Gbps QPSK signal at $V = 12 \pm 2$ m, whereas the SIL QD-DWL source displayed $V = 16 \pm 2$ m. Hence, again a minor performance difference between both sources is noted, with SIL QD-DWL exhibiting an additional $\sim 2 \pm 2$ m visibility range to reach the FEC, which becomes trivial when incorporating the error margin. This observation is in good agreement with the clear weather condition discussed in the previous section, suggesting both locking techniques based sources experiencing similar signal attenuation and distortion under dusty weather conditions. This investigation further supports the

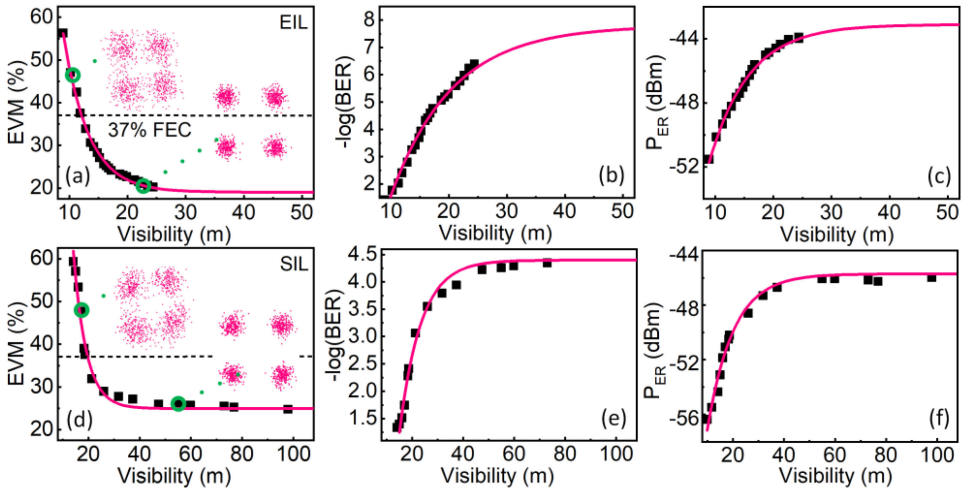

Fig. 6. Performance of link L_4: HY-FSO (20 km SMF, 0.9 m FSOD and 1 m WL) under dust storm effect for EVM, BER, and received electrical power, as a function of visibility range, shown in (a)–(c) for EIL QD-DWL and (d)–(f) for SIL QD-DWL. The respective constellation diagrams at two extreme values of visibility range are shown in the insets of (a) and (d).

potential of SIL QD-DWL as a candidate MMW source for future L-band optical networks and self-injection locking as a promising complementing technique compared to the energy-hungry external injection locking. Moreover, as seen from Fig. 6, both sources' performance improves with increasing V since dust particles start to settle down with time, thereby decreasing the particle density contained in the air and eventually saturating at $V = \sim$50–100 m. To further infer the system performance under moderate dust conditions, the data points of Fig. 6 are fitted with an exponential curve as this trend has been observed in the literature [5], [8]. It is worth mentioning here that for an accurate fitting, the clear case data point (before start) tabulated in Table 2 is incorporated and placed at a large V value during fitting since this value would eventually be achieved after some time. Thus, the moderate dust condition results are acquired from the saturated region of the fitted curves (i.e., between 0.2 km $< V \leq$ 1.0 km) for both EIL and SIL cases and are tabulated in Table 2. As expected, the decrease in EVM to 19% and 23% is noted for the EIL and SIL QD-DWL, and ~5.5 dBm improvement in P_{ER} in both cases, compared to the dense dust condition FEC value. Insets in Fig. 6(a) and (d) show the received QPSK constellation for two extreme V values compared to the FEC threshold highlighting the improved performance with increasing V. Moreover, observe that the data of Table 2 displays slightly better BER, EVM, and P_{ER} values compared to the SIL counterpart, whereas the latter system exhibited a relatively better V without considering the error margins. Hence, considering all these performance variables, which have been fitted independently despite being interdependent (EVM, BER, and P_{ER}), dictates comparable performance from both systems, with EIL probably performing slightly better, which could be from the generated MMW beat-tone carrier quality.

4. Conclusion

In summary, we experimentally demonstrated 30 GHz MMW photonic signal generation employing two QD-DWL sources emitting in ~1610 nm, which are based on EIL and SIL techniques. Later, successful 2 Gbps QPSK signal transmission over 30 GHz MMW beat-tone on WL, hybrid-WL, and hybrid-RoFSO channels is demonstrated under clear weather conditions utilizing both the injection-locked QD-DWL sources showing slightly better performance from the EIL source. Moreover, a rigorous analysis under dusty weather conditions revealed $V = 12 \pm 2$ m and 16 ± 2 m, from

EIL and SIL-DWL sources, respectively. In general, the attractive features of simple, cost-effective, and energy-efficient SIL QD-DWL, along with similar performance characteristics, compared to the EIL counterpart, and demonstration in challenging mid L-band rather than typical C-band, highlight promising outlook of this source for next-generation optical networks, besides self-injection locking as a candidate scheme.

References

[1] L. Vallejo *et al*., "Impact of thermal-induced turbulent distribution along FSO link on transmission of photonically generated mmW signals in the frequency range 26–40 GHz," *IEEE Photon. J*., vol. 12, no. 1, Feb. 2020.

[2] J. Bohata *et al*., "24–26 GHz radio-over-fiber and free-space optics for fifth-generation systems," *Opt. Lett.,* vol. 43, no. 5, pp. 1035–1038, 2018.

[3] X. Ge, S. Tu, G. Mao, C. Wang, and T. Han, "5G Ultra-dense cellular networks," *IEEE Wireless Commun*., vol. 23, no. 1, pp. 72–79, Feb. 2016.

[4] H. Wang, C. Cheng, C. Tsai, Y. Chi, and G. Lin, "Multi-color laser diode heterodyned 28-GHz millimeter-wave carrier encoded with DMT for 5G wireless mobile networks," *IEEE Access*, vol. 7, pp. 122697–122706, 2019.

[5] M. A. Esmail. A. M. Ragheb, H. A. Fathallah, M. Altamimi, and S. A. Alshebeili, "5G–28 GHz signal transmission over hybrid all-optical FSO/RF link in dusty weather conditions," *IEEE Access*, vol. 7, pp. 24404–24410, 2019.

[6] K. Su, L. Moeller, R. B. Barat, and J. F. Federici, "Experimental comparison of terahertz and infrared data signal attenuation in dust clouds," *J. Opt. Soc. Amer. A*, vol. 29, no. 11, pp. 2360–2366, 2012.

[7] J. Libich *et al*., "Combined effect of turbulence and aerosol on free-space optical links," *Appl. Opt*., vol. 56, no. 2, pp. 336–341, Jan. 2017.

[8] M. A. Esmail, H. Fathallah, and M. Alouini, "An experimental study of FSO link performance in desert environment," *IEEE Commun. Lett*., vol. 20, no. 9, pp. 1888–1891, Sep. 2016.

[9] C-Y. Lin *et al*., "Millimeter-wave carrier embedded dual-color laser diode for 5G MMW of link," *J. Lightw. Technol*., vol. 35, no. 12, pp. 2409–2420, 2017.

[10] M. A. Shemis *et al*., "Broadly tunable self-injection locked InAs/InP quantum-dash laser based fiber/FSO/hybrid fiber FSO communication at 1610 nm," *IEEE Photon. J*., vol. 10, no. 2, Feb. 2017, Art. no. 7902210.

[11] Q. Tareq *et al*., "Wireless transmission of millimeter waves generated by L-band InAs/InP quantum-dash laser," in *Proc. IEEE Photon. Conf*., Vancouver, BC, Canada, 2020, pp. 1–2.R. Lang.

[12] F. van Dijk, A. Accard, A. Enard, O. Drisse, D. Make, and F. Lelarge, "Monolithic dual wavelength DFB lasers for narrow linewidth heterodyne beat-note generation," in *Proc. Int. Topical Meeting Microw. Photon. Jointly Held Asia-Pacific Microwave Photon. Conference*, Singapore, 2011, pp. 73–76.

[13] M. Rahim *et al*., "Monolithic InAs/InP quantum dash dual-wavelength DFB laser with ultra-low noise common cavity modes for millimeter-wave applications," *Opt. Express*, vol. 27, no. 24, pp. 35368–35375, 2019.

[14] K. Zeb *et al.,* "Ultra-low intensity and phase noise quantum-dash dual-wavelength dfb laser for 5G millimeter-wave signals," in *Proc. Laser Appl. Conf. Opt. Soc. Amer*., 2020, Paper JTu5A.13.

[15] H. H. Elwan, R. Khayatzadeh, J. Poette, and B. Cabon, "Impact of relative intensity noise on 60-ghz radio-over-fiber wireless transmission systems," *J. Lightw. Technol*., vol. 34, no. 20, pp. 4751–4757, Oct. 2016.

[16] T. Shao *et al*., "Chromatic dispersion-induced optical phase decorrelation in a 60 GHz ofdm-rof system," *IEEE Photon. Technol. Lett*., vol. 26, no. 20, pp. 2016–2019, Oct. 2014.

[17] C. Tsai, Cheng-Ting, C.-H. L., C.-T. Lin, Y.-C. Chi, and G.-R. Lin. "60-GHz millimeter-wave over fiber with directly modulated dual-mode laser diode," *Sci. Rep.,* vol. 6, no. 1, pp. 1–12, 2016.

[18] J. L. Li, F. Zhao, and J. Yu, "D-band millimeter wave generation and transmission though radio-over-fiber system," *IEEE Photon. J*., vol. 12, no. 2, Apr. 2020, Art. no. 5500708.

[19] R. A. Shafik, M. S. Rahman, A. R. Islam, and N. S. Ashraf, "On the error vector magnitude as a performance metric and comparative analysis," in *Proc. Int. Conf. Emerg. Technol*., Peshawar, Pakistan, 2006, pp. 27–31.